Unifying Sequential Quadratic Programming and Linear-Parameter-Varying Algorithms for Real-Time Model Predictive Control

Kristóf Floch, Amon Lahr, Roland Tóth, and Melanie N. Zeilinger

Abstract—This paper presents a unified framework that connects sequential quadratic programming (SOP) and the iterative linear-parameter-varying model predictive control (LPV-MPC) technique. Using the differential formulation of the LPV-MPC, we demonstrate how SQP and LPV-MPC can be unified through a specific choice of scheduling variable and the 2nd Fundamental Theorem of Calculus (FTC) embedding technique and compare their convergence properties. This enables the unification of the zero-order approach of SQP with the LPV-MPC scheduling technique to enhance the computational efficiency of stochastic and robust MPC problems. To demonstrate our findings, we compare the two schemes in a simulation example. Finally, we present real-time feasibility and performance of the zeroorder LPV-MPC approach by applying it to Gaussian process (GP)-based MPC for autonomous racing with real-world experiments.

I. Introduction

Supported by advances in numerical optimization, model predictive control (MPC) has become a key technique for the safety-critical control of dynamical systems due to its ability to handle constraints and its predictive capabilities [1]. As most real-world processes exhibit nonlinear behavior, nonlinear MPC (NMPC) has received increasing attention in recent years [2]. To compute the NMPC input, a nonlinear program (NLP) needs to be solved at every sampling time. For this, the two most popular techniques are based on interior point methods and sequential quadratic programming (SQP) [3]. Particularly, SQP methods have gained significant attention in recent years for NMPC problems [4]. In SQP, the solution of an NLP is approximated by iteratively solving a sequence of quadratic programs (QPs). The primary advantage of using QPs is their convexity, which allows the use of efficient solvers capable of providing real-time solutions [4]. Furthermore, real-time iteration schemes (RTI) [5] can enable embedded implementation of the control law. However, the application of SQP algorithms still has limitations: as it linearizes the constraints, it is sensitive to initialization.

Closely related to the SQP algorithm, [6] proposes a quasilinear MPC framework that embeds a nonlinear system into a *linear parameter-varying* (LPV) form, allowing the NMPC problem to be solved by successive solution of linear MPC

K. Floch, A. Lahr and M. Zeilinger are with the Inst. for Dynamic Systems and Control, ETH Zürich, Zürich, Switzerland {kfloch, amlahr, mzeilinger}@ethz.ch. R. Tóth is with the Control Systems Group, Eindhoven University of Technology, Eindhoven, The Netherlands and the Systems and Control Lab, HUN-REN Inst. for Computer Science and Control, Budapest, Hungary r.toth@tue.nl.

problems, corresponding to QPs. In subsequent sections, this method will be referred to as LPV-MPC. Comparing LPV-MPC with SQP, it can be demonstrated that the two methods have similar convergence properties if the LPV model is obtained by linearization [7]. More recently, [8], utilizes an automatic FTC-based embedding technique [9], to achieve a global LPV representation without approximation. However, the relation of this FTC-based iterative LPV-MPC scheme to SQP has not been thoroughly investigated, and it is yet to be deployed in real hardware experiments.

To further enhance the real-time capabilities of SQP, [10], [11] propose a zero-order scheme, where a subset of the states of the system is decoupled from the *optimal control problem* (OCP), through a tailored Jacobian approximation. This approach was shown to be particularly beneficial for robust [11], stochastic [10] and GP-based [12] NMPC (GP-MPC) schemes, where decoupling the uncertainty propagation from the OCP leads to the elimination of the quadratic scaling of the number of optimization variables on the system states. Similarly, in the LPV literature, scheduling variables have been utilized to eliminate state variables from the OCP for GP-MPC [13]. However, these approaches are yet to be compared and unified.

The main contributions of this paper are as follows:

- C1 We introduce a unified solution method for NMPC problems for which the SQP and the FTC-based LPV-MPC schemes are sub-cases. In particular, we show that the FTC embedding approach for LPV-MPC recovers SQP under a specific choice of so-called anchor points.
- C2 We show that the zero-order approximation of the Jacobians can be integrated into the unified scheme and how it can be viewed as using an extended scheduling variable in the LPV-MPC variant.
- C3 We compare computational complexity and the convergence properties of SQP and LPV-MPC in simulation.
- C4 We apply the unified zero-order scheme for the learning-based control of autonomous race cars. Specifically, we implement both the SQP and LPV-based version of the zero-order GP-MPC algorithm [12] in L4ACADOS [14] to solve the *model predictive contouring control* (MPCC) problem in simulation and real-world experiments.

The remainder of this paper is structured as follows. Sec. II reviews NMPC, introducing both SQP and iterative LPV-MPC as the basis for this paper. Sec. III develops a unified

framework that combines the two approaches through a differential formulation and unifies the zero-order method. Then, Sec. IV presents a simulation study, highlighting convergence behavior and computational complexity as well as the applicability of the method for autonomous racing. Finally, Sec. V complements these results with experimental validation.

II. NONLINEAR MPC

A. General NMPC Problem

We consider a general discrete-time (DT) nonlinear (NL) system of the form

$$x[k+1] = f(x[k], u[k]), (1)$$

where $x[k] \in \mathbb{R}^{n_{\mathbf{x}}}$ is the state vector, $u[k] \in \mathbb{R}^{n_{\mathbf{u}}}$ is the input vector, and $k \in \mathbb{N}$ denotes the discrete time step. The DT state evolution is defined by $f : \mathbb{R}^{n_{\mathbf{x}}} \times \mathbb{R}^{n_{\mathbf{u}}} \to \mathbb{R}^{n_{\mathbf{x}}}$.

For simplicity, as a control objective, we focus on stabilizing the system around an equilibrium point, assumed w.l.o.g. to be at the origin. However, we note that the extension to tracking tasks is straightforward, see [1]. Furthermore, we prescribe state and input constraints as $h(x[k],u[k]) \leq 0$, $h_N(x[k]) \leq 0$, where $h: \mathbb{R}^{n_x} \times \mathbb{R}^{n_u} \to \mathbb{R}^{n_h}$, and $h_N: \mathbb{R}^{n_x} \to \mathbb{R}^{n_{h_N}}$.

Generally, in NMPC, given a current state measurement x[k] at time step k, an NLP is solved to obtain a sequence of optimal state and input values over a finite prediction horizon. The NLP can be formulated as follows:

$$\min_{X,U} \quad \sum_{i=0}^{N-1} l_i(x_i, u_i) + l_N(x_N)$$
 (2a)

s.t.
$$\forall i \in \mathbb{I}_0^{N-1}$$
 (2b)

$$x_{i+1} = f(x_i, u_i), \tag{2c}$$

$$h(x_i, u_i) < 0, (2d)$$

$$h_N(x_N) \le 0, \tag{2e}$$

$$x_0 = x[k], (2f)$$

where $l_i: \mathbb{R}^{n_{\mathrm{x}}} \times \mathbb{R}^{n_{\mathrm{u}}} \to \mathbb{R}$ denotes the stage cost, $l_N: \mathbb{R}^{n_{\mathrm{x}}} \to \mathbb{R}$ is the terminal cost, N is the control horizon, $U = [u_0^\top \dots u_{N-1}^\top]^\top$ and $X = [x_0^\top \dots x_N^\top]^\top$ are the optimization variables and $\mathbb{I}_{\tau_1}^{\tau_2} = \{i \in \mathbb{Z} \mid \tau_1 \leq i \leq \tau_2\}$. For simplicity, in this paper we consider quadratic stage and terminal costs defined as

$$l_i(x_i, u_i) \doteq ||x_i||_Q^2 + ||u_i||_R^2, \quad l_N(x_N) \doteq ||x_N||_W^2,$$
 (3)

where $Q \succeq 0$, $R \succ 0$, and $W \succeq 0$ are the positive (semi-)definite weighting matrices and $\|a\|_B^2 \doteq a^\top B a$. In the following, we assume that all functions in the NLP (2) are at least twice continuously differentiable.

B. SQP Solution

The main idea of the SQP-based solution is that, given an initial guess of $\hat{X} = [\hat{x}_0^\top \dots \hat{x}_N^\top]^\top$, $\hat{U} = [\hat{u}_0^\top \dots \hat{u}_{N-1}^\top]^\top$, the original problem (2) is approximated by a single QP, which provides a reliable approximation in a local neighborhood around the linearization point \hat{X}, \hat{U} . By defining the optimization variables as $\Delta x_i = x_i - \hat{x}_i$, $\Delta u_i = u_i - \hat{u}_i$,

the QP yields $\Delta X^{\star}, \Delta U^{\star}$. Then, the current approximation is updated as $\hat{X} \leftarrow \hat{X} + \Delta X^{\star}$, $\hat{U} \leftarrow \hat{U} + \Delta U^{\star}$ to obtain a sequence of solutions that is, under certain conditions, proven to converge to a Karush-Kuhn-Tucker (KKT) point of (2), denoted by X^{\star}, U^{\star} , cf. [15, Thm. 1]. The quadratic subproblem solved at each SOP iteration can be defined as

$$\min_{\Delta X, \Delta U} \sum_{i=0}^{N-1} \frac{1}{2} \begin{bmatrix} \Delta x_i \\ \Delta u_i \end{bmatrix}^{\top} \mathcal{M}_i \begin{bmatrix} \Delta x_i \\ \Delta u_i \end{bmatrix} + m_i^{\top}(\hat{x}_i, \hat{u}_i) \begin{bmatrix} \Delta x_i \\ \Delta u_i \end{bmatrix} + \frac{1}{2} \Delta x_N^{\top} \mathcal{M}_N \Delta x_N + m_N^{\top}(\hat{x}_N) \Delta x_N \tag{4a}$$

s.t.
$$\forall i \in \mathbb{I}_0^{N-1}$$
, (4b)

$$\Delta x_{i+1} = A_i \Delta x_i + B_i \Delta u_i + \Delta W_i^{\mathbf{x}}, \tag{4c}$$

$$0 > H_i^{\mathbf{x}} \Delta x_i + H_i^{\mathbf{u}} \Delta u_i + \Delta \mathcal{W}_i^{\mathbf{h}}, \tag{4d}$$

$$0 > H_N^{\mathbf{x}} \Delta x_N + \Delta \mathcal{W}_N^{\mathbf{h}},\tag{4e}$$

$$\Delta x_0 = 0. (4f)$$

In the cost of (4), \mathcal{M}_i is the chosen approximation of the Hessian of the Lagrangian and m_i is the Jacobian of the original cost at step i. The derivation of \mathcal{M}_i is included in Appendix A. The state and input matrices for the linearized dynamics and constraints are the Jacobians of (2c) and (2d) (2e), respectively, evaluated at \hat{x}, \hat{u} , i.e.,

$$A_{i} = \frac{\partial f}{\partial x}\Big|_{\substack{\hat{x}_{i} \\ \hat{u}_{i}}}, B_{i} = \frac{\partial f}{\partial u}\Big|_{\substack{\hat{x}_{i} \\ \hat{u}_{i}}}, H_{i}^{x} = \frac{\partial h}{\partial x}\Big|_{\substack{\hat{x}_{i} \\ \hat{u}_{i}}}, H_{i}^{u} = \frac{\partial h}{\partial u}\Big|_{\substack{\hat{x}_{i} \\ \hat{u}_{i}}},$$
(5)

and the residual terms are

$$\Delta \mathcal{W}_i^{\mathbf{x}} = f(\hat{x}_i, \hat{u}_i) - \hat{x}_{i+1},\tag{6a}$$

$$\Delta \mathcal{W}_i^{\text{h}} = h(\hat{x}_i, \hat{u}_i), \ i \in \mathbb{I}_0^{N-1}, \ \Delta \mathcal{W}_N^{\text{h}} = h(\hat{x}_N). \tag{6b}$$

Using (4), the standard SQP algorithm is summarized in Alg. 1. In particular, if the solution of the quadratic subproblem yields a vanishing step $\Delta X=0$, $\Delta U=0$, then, according to Lemma 2.1, the current iterate satisfies the KKT conditions of the original nonlinear program.

Algorithm 1 SQP-based MPC.

- 1: **input** x[k] (measured state at time k), X^*, U^* (optimal state/input sequence at time k-1)
- 2: initialize $\hat{X} = X^*, \hat{U} = U^*$
- 3: repeat
- 4: **set** $A_i, B_i, i \in \mathbb{I}_{i=0}^{N-1}$ via (5)
- 5: **solve** (4) to obtain $\Delta X^*, \Delta U^*$
- 6: **update** $\hat{X} := \hat{X} + \Delta X^{\star}, \ \hat{U} := \hat{U} + \Delta U^{\star}$
- 7: until convergence criterion is reached
- 8: **set** $X^* = \hat{X}, \ U^* = \hat{U}$
- 9: **apply** $u[k] = [U^{\star}]_0$

Lemma 2.1 (Optimality of SQP [3, Chap. 18]):

Consider the NMPC problem (2), solved by SQP using Alg. 1. Suppose that standard SQP assumptions hold [15, Sec. 3.1] and the algorithm has converged, i.e., $\Delta X^{\star}=0,\ \Delta U^{\star}=0.$ Then, X^{\star},U^{\star} together with the corresponding Lagrange multipliers (λ,μ) satisfy the KKT

first-order optimality conditions of the original NLP (2), in particular, X^*, U^* is a first-order stationary point of the NLP, i.e., a locally optimal solution.

During optimization, KKT residuals of the original NLP (2) are commonly used as a convergence criterion for SQP implementations [3, Eq. (12.34)].

C. Iterative LPV-MPC

An alternative approach to solve (2) is to utilize an LPV embedding in an iterative LPV-MPC scheme [6]. To discuss this approach, first, the LPV embedding of NL systems is outlined using the FTC, based on [9]. Then, the iterative solution of the LPV-MPC problem is presented.

1) LPV systems: A wide class nonlinear functions can be represented as $f(x,u) = A(\Phi(x,u))x + B(\Phi(x,u))u + V$, where $A: \mathbb{R}^{n_{\rho}} \to \mathbb{R}^{n_{\mathbf{x}} \times n_{\mathbf{x}}}$, $B: \mathbb{R}^{n_{\rho}} \to \mathbb{R}^{n_{\mathbf{x}} \times n_{\mathbf{u}}}$ are matrices depending on the states and inputs via the so-called scheduling map $\Phi: \mathbb{R}^{n_{\mathbf{x}}} \times \mathbb{R}^{n_{\mathbf{u}}} \to \mathbb{R}^{n_{\rho}}$. By defining the scheduling variable as $\rho[k] \doteq \Phi(x[k], u[k])$ the LPV representation [16] of (1) can be expressed as

$$x[k+1] = A(\rho[k])x[k] + B(\rho[k])u[k] + V, \tag{7}$$

where the dependence of ρ on x and u is either intentionally omitted to obtain an embedding of the NL system enabling convex analysis and synthesis, or treated as a known or uncertain sequence in predictive control. The exists a large variety of methods to accomplish the factorization of the nonlinearity to obtain the LPV representation (7). Many of these methods are only applicable for specific cases, computationally demanding, or require expert decisions in the modeling process. In this paper, we focus on the FTC-based formulation proposed by [9], whose benefit is that it provides the embedding of the exact nonlinear dynamics into an LPV representation automatically.

Given a continuously differentiable function $a: \mathbb{R}^n \to \mathbb{R}^m$, the FTC states that, for $\eta, \tilde{\eta} \in \mathbb{R}^n$,

$$a(\eta) - a(\tilde{\eta}) = \left(\int_0^1 \frac{\mathrm{d}a}{\mathrm{d}\eta} \Big|_{\tilde{\eta} + \lambda(\eta - \tilde{\eta})} \mathrm{d}\lambda \right) (\eta - \tilde{\eta}), \quad (8)$$

where $\left. \frac{\mathrm{d}a}{\mathrm{d}\eta} \right|_{\lambda\eta}$ is the Jacobian of a evaluated at $\lambda\eta$. Since f is differentiable, by choosing $\eta_i = [x_i^\top \ u_i^\top]^\top$ and $\tilde{\eta} = [\tilde{x}_i^\top \ \tilde{u}_i^\top]^\top$, we obtain

$$f(x_{i}, u_{i}) = \underbrace{\int_{0}^{1} \frac{\partial f}{\partial x} \Big|_{\substack{\tilde{x}_{i} + \lambda(x_{i} - \tilde{x}_{i}) \\ \tilde{u}_{i} + \lambda(u_{i} - \tilde{u}_{i})}} d\lambda(x_{i} - \tilde{x}_{i})}_{\bar{A}(x_{i}, u_{i})} + \underbrace{\int_{0}^{1} \frac{\partial f}{\partial u} \Big|_{\substack{\tilde{x}_{i} + \lambda(x_{i} - \tilde{x}_{i}) \\ \tilde{u}_{i} + \lambda(u_{i} - \tilde{u}_{i})}}}_{\bar{B}(x_{i}, u_{i})} d\lambda(u_{i} - \tilde{u}_{i}) + V_{i}, \quad (9)$$

where $V_i = f(\tilde{x}_i, \tilde{u}_i)$ is a term dependent on the anchor points \tilde{x}_i, \tilde{u}_i . By defining the scheduling map as $\Phi(x_i, u_i) \doteq [x_i^\top u_i^\top]^\top$, the scheduling-dependent

state and input matrices of the LPV form become $A(\rho_i) \doteq \bar{A}(x_i, u_i), \quad B(\rho_i) \doteq \bar{B}(x_i, u_i).$ Note that in most LPV applications, the anchor points \tilde{x}_i, \tilde{u}_i are considered constant-zero with 0 = f(0,0), which naturally gives the LPV form. In contrast, this paper also investigates non-zero and varying anchor points along the prediction horizon. It is also important to highlight that, for the LPV conversion, the calculation of the integrals of the Jacobians is required. While the Jacobians can be easily computed using symbolic computation packages or algorithmic differentiation, the analytical expression of the integrals is a difficult task. However, as only the values of the A and B matrices are interesting in an MPC formulation at a given $\rho[k]$, we can rely on numerical integration methods, which can also be parallelized [8] for efficiency. Note that it is straightforward to extend (8) to nonlinear inequality constraints, yielding a similar parameter-varying formulation.

2) LPV-MPC: Using the LPV model obtained in Sec. II-C.1, we can employ the method outlined in [6] to solve the NMPC problem efficiently using an iterative procedure. The key idea of the LPV-MPC approach is that at any given time step k, for a fixed scheduling sequence $P = [\rho_0^\top \dots \rho_{N-1}^\top]^\top$, Eq. (7) reduces to an affine system, for which the MPC problem can be efficiently solved via a QP. The quadratic subproblem is characterized as

$$\min_{X,U} \sum_{i=0}^{N-1} (\|x_i\|_Q^2 + \|u_i\|_R^2) + \|x_N\|_W^2,$$
 (10a)

$$\text{s.t. } \forall i \in \mathbb{I}_0^{N-1} \tag{10b}$$

$$x_{i+1} = A(\rho_i)(x_i - \tilde{x}_i) + B(\rho_i)(u_i - \tilde{u}_i) + V_i^{x},$$
(10c)

$$0 \ge H^{\mathbf{x}}(\rho_i)(x_i - \tilde{x}_i) + H^{\mathbf{u}}(\rho_i)(u_i - \tilde{u}_i) + V_i^{\mathbf{h}},$$
(10d)

$$0 \ge H^{\mathbf{x}}(\rho_N)(x_N - \tilde{x}_N) + V_N^{\mathbf{h}},$$
 (10e)

$$x_0 = x[k]. ag{10f}$$

As P is fixed in (10), the state propagation reduces to LTV dynamics. Furthermore, (10d) is the LPV factorization of the constraints (2d) . As a result, (10) corresponds to a quadratic subproblem which can be efficiently solved by off-the-shelf QP solvers [4]. Solving (10) yields the optimal input sequence U^* , which can be used to forward-simulate the NL model (1) to obtain the scheduling sequence at time step k+1, based on which a new quadratic subproblem can be formulated and solved. By executing this iteration until the input trajectory has converged, the solution of the quadratic subproblem converges to a suboptimal solution of the NMPC, assuming that the LPV approximation is sufficiently accurate, according to Lemma 2.2.

Lemma 2.2 (Suboptimality of LPV–MPC [7, Thm. 3]): Consider the LPV–MPC problem (10), with a scheduling trajectory $\rho_i = \Phi(\hat{x}_i, \hat{u}_i)$ forming the QP approximation according to (10) and Alg. 2. Suppose the algorithm has converged, i.e., the solution (X^\star, U^\star) of the QP coincides with the current iterate. Then (X^\star, U^\star) is feasible and in general a suboptimal solution for the original NMPC (2).

The iterative LPV-MPC algorithm is outlined in Alg. 2.

Algorithm 2 Iterative LPV-MPC.

1: **input** x[k] (measured state at time k), U^* (optimal input sequence at k-1)

2: initialize $[P]_i = \Phi(x[k], [U^{\star}]_{i+1}), i \in \mathbb{I}_{i-0}^{N-1}$

set $A(\rho_i), B(\rho_i), i \in \mathbb{I}_{i=0}^{N-1}$ via (9)

solve (10) to obtain ${\cal U}$ 5:

 $\begin{array}{l} \textbf{simulate} \ (1) \ \text{with} \ U^\star \leftarrow U \ \text{and} \ x[k] \ \text{to obtain} \ X \\ \textbf{set} \ [P]_i = \rho_i = \Phi([X]_i, [U]_i), \ i \in \mathbb{I}_{i=0}^{N-1} \end{array}$

8: **until** P has converged

9: **apply** $u[k] = [U^{\star}]_0$

As convergence criterion, most LPV-MPC approaches monitor the convergence of the scheduling variables, i.e., if

$$\|P - \hat{P}\|_{\infty} \le \epsilon_{\text{LPV}},$$
 (11)

where \hat{P} denotes the scheduling sequence from the previous LPV iteration and $\|\cdot\|$ is the L_{∞} norm.

III. UNIFYING SQP AND LPV-MPC

A. Equivalence Condition

To show how the SQP and LPV-MPC approaches are related, we reformulate the OP of the LPV-MPC problem into a differential form akin to SQP, i.e., we use ΔX and ΔU as optimization variables, similarly to [17]. First, along the trajectory \hat{X}, \hat{U} , the state-evolution constraint (10c) can be expressed as

$$x_{i+1} = A(\hat{\rho}_i)x_i + B(\hat{\rho}_i)u_i + \mathcal{W}_i^{\mathbf{x}} \tag{12}$$

with $W_i = V_i^{\mathrm{x}} - A(\hat{\rho}_i)\tilde{x}_i - B(\hat{\rho}_i)\tilde{u}_i$, which is completely determined by the stage-wise anchor points X, U and the trajectory \hat{X}, \hat{U} . By defining $\Delta x_i := x_i - \hat{x}_i, \ \Delta u_i := u_i - \hat{u}_i$, we arrive at

$$\hat{x}_{i+1} + \Delta x_{i+1} = A(\hat{\rho}_i) \Delta x_i + B(\hat{\rho}_i) \Delta u_i$$

$$+ A(\hat{\rho}_i) \hat{x}_i + B(\hat{\rho}_i) \hat{u}_i + \mathcal{W}_i^{\mathbf{x}}.$$

$$(13)$$

Finally, by rearranging the terms, the state propagation in differential form can be expressed as

$$\Delta x_{i+1} = A(\hat{\rho}_i) \Delta x_i + B(\hat{\rho}_i) \Delta u_i + \Delta \mathcal{W}_i^{\mathbf{x}}, \qquad (14)$$

where the residual term is

$$\Delta W_i^{\mathbf{x}} = -\hat{x}_{i+1} + \underbrace{A(\hat{\rho}_i)(\hat{x}_i - \tilde{x}_i) + B(\hat{\rho}_i)(\hat{u}_i - \tilde{u}_i) + V_i^{\mathbf{x}}}_{f(\hat{x}_i, \hat{u}_i)},$$
(15)

according to the FTC-based factorization (9).

Finally, we outline a general unified notation that can be employed for both the SQP and the LPV-MPC methods by

introducing the following standard quadratic form:

$$\min_{\Delta X, \Delta U} \quad \sum_{i=0}^{N-1} \frac{1}{2} \begin{bmatrix} \Delta x_i \\ \Delta u_i \end{bmatrix}^\top \mathcal{M}_i \begin{bmatrix} \Delta x_i \\ \Delta u_i \end{bmatrix} + \left(M_i \begin{bmatrix} \hat{x}_i \\ \hat{u}_i \end{bmatrix} \right)^\top \begin{bmatrix} \Delta x_i \\ \Delta u_i \end{bmatrix}$$

$$+\frac{1}{2}\Delta x_N^{\mathsf{T}} \mathcal{M}_N \Delta x_N + (M_N \hat{x}_N)^{\mathsf{T}} \Delta x_N \tag{16a}$$

s.t.
$$\forall i \in \mathbb{I}_0^{N-1}$$
 (16b)

$$\Delta x_{i+1} = A_i \Delta x_i + B_i \Delta u_i + \Delta W_i^{\mathbf{x}}, \tag{16c}$$

$$0 \ge H_i^{\mathbf{x}} \Delta x_i + H_i^{\mathbf{u}} \Delta u_i + \Delta \mathcal{W}_i^{\mathbf{h}}, \tag{16d}$$

$$0 \ge H_N^{\mathbf{x}} \Delta x_N + \Delta \mathcal{W}_N^{\mathbf{h}},\tag{16e}$$

$$\Delta x_0 = 0. \tag{16f}$$

In SOP, \mathcal{M}_i denotes the approximated Hessian of the Lagrangian corresponding to stage i (see Appendix A), while for the LPV-MPC, $\mathcal{M}_i = M_i = \operatorname{diag}(Q, R)$, for all $i \in \mathbb{I}_0^{N-1}$ and $\mathcal{M}_N = M_N = W$, i.e., it is composed of the weighting matrices of the MPC cost. Note that by employing Gauss-Newton approximation for SQP [18, Sec. 3.1], we retrieve the same block diagonal matrix, as the approximation neglects the dependence of the Lagrangian on the constraints. In both cases, $M_i = diag(Q, R)$. To get a better overview, all the parameters of (16) are collected in Table I. In conclusion, it is important to emphasize that the LPV iterations use the integrated Jacobians as transition matrices to obtain the exact embedding of the nonlinear dynamics, whereas the SQP methods rely on the Jacobians obtained through linearization.

The unified formulation directly yields the following results.

Proposition 3.1 (Equivalence of SQP and LPV-MPC): Consider the LPV-MPC formulation (10) with the FTCbased LPV embedding. If the stage-wise anchor points are chosen as the previous solutions, i.e., $\tilde{x}_i = \hat{x}_i$, $i \in \mathbb{I}_0^N$, $\tilde{u}_i = \hat{u}_i, \ i \in \mathbb{I}_0^{N-1}$, then the LPV-MPC iteration coincides exactly with the SQP iteration for the original nonlinear MPC problem. Consequently, at convergence, the solution

Proof: When the anchor points are set as $\tilde{x}_i = \hat{x}_i$ and $\tilde{u}_i = \hat{u}_i$, the LPV system and constraint matrices computed by (9) reduce to the Jacobians of (2c) and (2d), respectively. Consequently, both the equality constraints and the inequality constraints in (16) coincide exactly with the first-order Taylor expansions used in SQP. Therefore, the LPV-MPC step is equivalent to the SQP subproblem, and the standard SQP convergence results apply (see Lemma 2.1), ensuring local convergence to the optimal solution of the original NLP.

Corollary 3.2: Let X^* , U^* denote a KKT point of (2). If $\tilde{X} = X^{\star}, \ \tilde{U} = U^{\star}, \text{ then, } X^{\star}, \ U^{\star} \text{ is a stationary point of }$ the LPV-MPC algorithm (Alg. 2).

Proof: Let $\hat{X} = X^*$, $\hat{U} = U^*$, i.e., the solution of the last OP corresponds to the optimal solution. Then, since $\hat{X} = \tilde{X}$ and $\hat{U} = \tilde{U}$, according to Proposition 3.1, the next iterate coincides with the SQP solution. However, as the last solution corresponds to a KKT point of (2), the SQP step yields $\Delta X = 0$, $\Delta U = 0$, i.e., X^* , U^* is a stationary point of the LPV-MPC algorithm (Alg. 2).

¹For $i \geq 2$, X^* can also be used to initialize P.

TABLE I: Comparison of the QPs corresponding to the SQP and LPV-based NMPC solution methods.

Parameter	SQP	LPV-MPC		
\mathcal{M}_i	$\operatorname{diag}(Q,R)^2$	$\operatorname{diag}(Q,R)$		
M_i	$\operatorname{diag}(Q,R)^2$	diag(Q, R)		
A_i	$\frac{\partial f}{\partial x}\Big _{\substack{\hat{x}_i \\ \hat{u}_i}}$	$\int_0^1 \frac{\partial f}{\partial x} \Big _{\substack{\tilde{x}_i + \lambda(\hat{x}_i - \tilde{x}_i) \\ \tilde{u}_i + \lambda(\hat{u}_i - \tilde{u}_i)}} d\lambda$		
B_i	$\frac{\partial f}{\partial u}\Big _{\substack{\hat{x}_i \\ \hat{u}_i}}$	$\int_{0}^{1} \frac{\partial f}{\partial u} \Big _{\substack{\hat{x}_{i} + \lambda(\hat{u}_{i} - \tilde{u}_{i}) \\ \hat{u}_{i} + \lambda(\hat{u}_{i} - \tilde{u}_{i})}} d\lambda$		
ΔW_i^{x}	$f(\hat{x}_i, \hat{u}_i) - \hat{x}_{i+1}$	$f(\hat{x}_i, \hat{u}_i) - \hat{x}_{i+1}$		
$H_i^{\{\mathrm{x},\mathrm{u}\}}$	$\left. \frac{\partial h}{\partial \{x,u\}} \right _{\hat{u}_i}^{\hat{x}_i}$	$\int_0^1 \frac{\partial h}{\partial \{x, u\}} \Big _{\substack{\tilde{x}_i + \lambda(\hat{x}_i - \tilde{x}_i) \\ \tilde{u}_i + \lambda(\hat{u}_i - \tilde{u}_i)}} d\lambda$		
$\Delta W_i^{ m h}$	$h(\hat{x}_i, \hat{u}_i)$	$h(\hat{x}_i,\hat{u}_i)$		

B. Zero-order Approximation

For complex systems, it is often necessary to employ simplifications of the MPC scheme to ensure computational feasibility. A commonly used approach is to apply a zero-order approximation, where a tailored Jacobian structure allows one component of the state to be computed independently of the remaining variables, enabling it to be propagated outside the optimization problem, while the other components still depend on it within the optimization. This method has been successfully applied for robust [11] and stochastic [10], [12] MPC schemes to eliminate the uncertainty description from the optimization variables. In the following, we derive the zero-order approximation for the unified MPC description of Sec. III-A using the differential formulation.

Let the system states be divided as $x^{\top} = [y^{\top} z^{\top}]^{\top}$, where y are the states considered as optimization variables and z are the states to be propagated outside the optimization loop. Then the equality constraints corresponding to the state propagation (16c) can be formulated as

$$\begin{bmatrix} \Delta y_{i+1} \\ \Delta z_{i+1} \end{bmatrix} = \begin{bmatrix} A_i^{yy} & A_i^{yz} \\ A_i^{zy} & A_i^{zz} \end{bmatrix} \begin{bmatrix} \Delta y_i \\ \Delta z_i \end{bmatrix} + \begin{bmatrix} B_i^{y} \\ B_i^{z} \end{bmatrix} \Delta u_i + \begin{bmatrix} \Delta \mathcal{W}_i^{y} \\ \Delta \mathcal{W}_i^{z} \end{bmatrix}.$$
(17)

In the zero-order method, the following simplifications are made: $A_i^{\rm zy}=0,\,B_i^{\rm z}=0$. As a result, the evolution of z no longer depends on the optimization variables $\Delta x, \Delta u$ and can be simplified as

$$\Delta z_{i+1} = A_i^{zz} \Delta z_i + \Delta W_i^{z}, \tag{18}$$

where $\Delta W_i^z = -\hat{z}_{i+1} + f^z(\hat{y}_i, \hat{z}_i, \hat{u}_i)$ corresponds to the z-component of the original dynamics (1). As outlined in [10], there are multiple approaches to propagate the dynamics of z in between solver iterations. First, notice that $\Delta z_0 = 0$, (18) can be rolled out to obtain the sequence of auxiliary variables. Second, [10] also suggests the propagation of z based on the original nonlinear dynamics, i.e.,

$$z_{i+1} = f(\hat{y}_i, z_i, \hat{u}_i). \tag{19}$$

Note that if (19) is linear in the auxiliary variable z, the two methods produce identical results. Consequently, since most iterative LPV-MPC approaches addressing uncertainty (e.g. [13]) use this form of auxiliary propagation, they can be interpreted as a zero-order approximation known from the SQP scheme. The proposed unified framework thereby

allows to identify the correspondence and shows that the approximations introduced by i) the zero-order method in SQP and ii) the iterative LPV-MPC formulation that uses auxiliary state propagation (19) and an extended scheduling variable $\rho = [y^T \ u^T \ z^T]^T$ are equivalent.

IV. SIMULATION STUDY

Next, we compare the computational complexity and convergence properties of the SQP and the LPV-MPC algorithm through the proposed unified form, where the methods result as particular choices of the involved terms. For this, we have implemented both algorithms in ACADOS [2] using the L4ACADOS package [14]. The source code is available on GitHub³. All simulations are carried out using an M2 MacBook Air with 16 GB RAM.

First, we examine the convergence properties of both algorithms using a simplified nonlinear example; then, we employ both methods using RTI for the control of an autonomous race car.

A. Convergence Properties and Computational Complexity

First, we utilize the cart-pendulum system, see, e.g., [19, Eq. (23)-(24)], where p, \dot{p} are the position and velocity of the cart, and ϕ , $\dot{\phi}$ are the angle and angular velocity of the pendulum, jointly defining the state vector $x = [p \ \dot{p} \ \phi \ \dot{\phi}]^{\top}$. We aim to steer the system to the equilibrium $x^{eq} = 0$ from a downward initial position $x[0] = [0 \ 0 \ -\pi \ 0]^{\top}$. We consider box state and input constraints in the form $x_i \in [-5, 5] \times [-5, 5] \times [-2\pi, 2\pi] \times [-10, 10], u_i \in [-4, 4].$ To discretize the cart-pendulum system, we utilize a fourth-order Runge-Kutta (RK4) numerical integration method with $T_s = 0.01s$ sampling time. The prediction horizon is N = 20. Furthermore, for the LPV-MPC, we use a rectangular numerical integration scheme with $N_{\rm int}=20$ stages to compute the integral of the FTC-based embedding (9). To formulate the MPC cost (2a), we use Q = diag(100, 1, 100, 1), R = 10.

During the simulations, we compare five different LPV-MPC algorithms with the SQP scheme: (1) constant anchor points at the origin $\tilde{x}_i = 0$, $\tilde{u}_i = 0$; (2) constant nonzero⁴ anchor points $\tilde{x}_i = c^x$, $\tilde{u}_i = c^u$; (3) last input and measured state as anchor points $\tilde{x}_i = x[k]$, $\tilde{u}_i = u[k-1]^5$, with $u[-1] \doteq 0$; (4) last optimizer sequence as anchor points $\tilde{x}_i = \hat{x}_i$, $\tilde{u}_i = \hat{u}_i$; (5) optimal state and input sequence as anchor points $\tilde{x}_i = x_i^*$, $\tilde{u}_i = u_i^*$. For a fair comparison, both algorithms use the same initialization $\hat{x}_i = x[0]$, $\hat{u}_i = 0$.

In Fig. 1, we evaluate the NLP residuals of the original NMPC problem at the first time step by performing a fixed number of 10 iterations. As shown, the LPV-MPC algorithm generally converges to a suboptimal solution of the original NLP, according to Lemma 2.2. When the last optimizer

²Assuming Gauss-Newton Hessian approximation.

³https://gitlab.ethz.ch/ics/sqp_lpv_mpc

 $^{^4}$ The $c^{\rm x},c^{\rm u}$ values are picked randomly from the feasible set, then kept constant during the simulations.

⁵Note that this is different from gain-scheduled MPC, where the anchor points are 0 and the scheduling trajectory is set to be constant and equal to the previous state- and input-induced value.

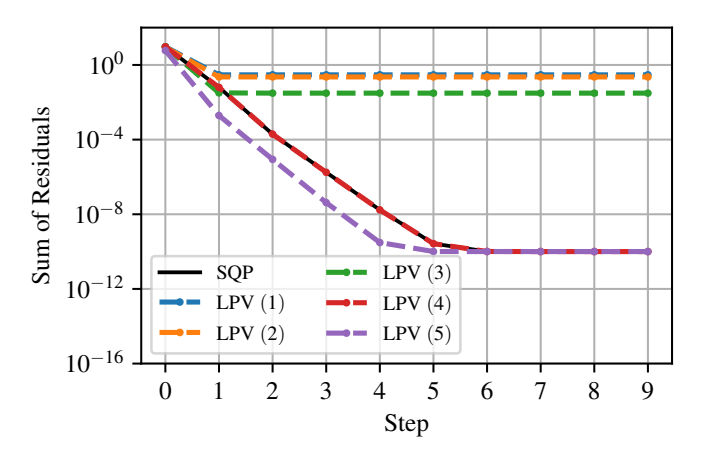


Fig. 1: KKT residuals of the SQP and LPV-MPC iterations for a single OCP for the cart-pendulum system.

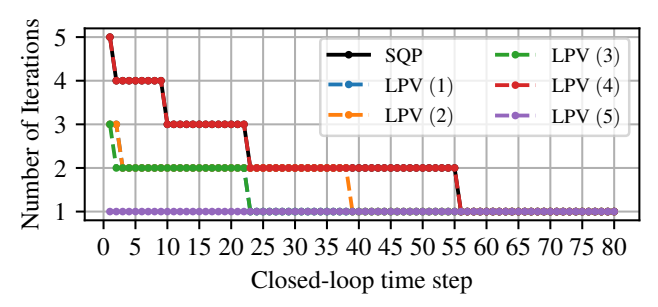


Fig. 2: Number of iterations required to converge at each closed-loop step for the cart-pendulum system. Note that the red line overlays the black.

sequence is used as the anchor sequence, we retain the SQP algorithm and its convergence properties, verifying Proposition 3.1. Furthermore, if the optimal control sequence is used as anchor points, the LPV-MPC converges to the optimal solution (Corollary 3.2), notably, faster than the SOP scheme.

In Fig. 2, the number of solver iterations required to converge is shown along a 80-step rollout of the closed-loop system. For a fair comparison, both algorithms use the same LPV-MPC termination criteria (11), with $\epsilon = 10^{-6}$. Note that this differs from the usual SQP termination criterion shown in Fig. 1 based on the KKT residuals.

Furthermore, Table II details the computational requirement of the preparation (construction of the QP) and the feedback (solving the QP) phases per iteration, averaged over the whole rollout. For this example, LPV-MPC approaches require fewer iterations to converge at the expense of suboptimality. The SQP algorithm generally needs more iterations to converge, however, because computing the Jacobian is cheaper than evaluating the integral (9), the total solution time remains comparable. However, it is important to note that for large-dimensional systems, where more QP iterations are expected, the LPV-MPC algorithm can be advantageous as the integration scheme (9) can be easily parallelized.

TABLE II: Computational times and number of iterations required to converge, averaged through the rollout for the autonomous racing simulation. Preparation time T_{prep} , feedback time $T_{\rm fb}$ are given in milliseconds, while $n_{\rm it}$ denotes the number of iterations.

Method	$(\tilde{x}_i.\ \tilde{u}_i)$	$T_{\rm prep}$	$T_{ m fb}$	$n_{ m it}$
SQP	-	0.53	0.46	2.09
LPV	(0, 0)	0.78	0.46	1.3
LPV	$(c^{\mathrm{x}}, c^{\mathrm{u}})$	0.79	0.46	1.5
LPV	(x[k], u[k-1])	0.76	0.45	1.28
LPV	$(\hat{x}_i, \ \hat{u}_i)$	0.75	0.46	2.09
LPV	$(x_i^{\star}, \ u_i^{\star})$	0.75	0.45	1

B. Autonomous Racing

This section applies the LPV-MPC algorithm for autonomous racing with MPCC [14], [20]. We first outline the autonomous ground vehicle (AGV) model and the resulting LPV-MPC formulation.

1) Vehicle Model: We use a dynamic single-track model [21, Eq. (5)] to describe the motion dynamics, where the state vector $x = [p_x \ p_y \ \psi \ v_x \ v_y \ \omega \ T \ \delta \ \theta]^\top$ comprises the 2D position of the vehicle (p_x, p_y) , heading angle ψ with respect to the global x-axis, longitudinal and lateral velocities (v_x, v_y) , and yaw rate ω in the body-fixed frame. Additionally T is the applied motor torque and δ is the steering angle. Lastly, θ is the progress along the track. Overall the model is obtained by combining of single track dynamics, a Pacejka tire model and integrators for the torque and steering dynamics and the progress variable. The control input is $u = [\dot{T} \dot{\delta} \dot{\theta}]^{\top}$, containing the time derivatives of the last three states. To obtain the DT dynamics for the MPCC formulation, we discretize the model by RK4 to obtain

$$x[k+1] = f_{\mathcal{C}}(x[k], u[k]). \tag{20}$$

2) LPV-MPCC formulation: The key idea of the MPCC algorithm is to maximize the progress along a predefined reference path while minimizing the deviation from it and respecting the constraints imposed by the boundaries of the reference track. To embed the MPCC formulation into the LPV-MPC framework, we define the output equation and the track constraints as

$$y_i = c(x_i), \tag{21}$$

$$0 \ge h(x_i, u_i),\tag{22}$$

where $y_i = [e_1 \ e_c]^{\top}$ are the contouring and lag errors [22, Sec. IV.B]. Then, using the FTC-based embedding for (21), (20) and (22) with scheduling variable $\rho_i = [x_i^\top u_i^\top]^\top$, the OCP of the LPV-MPCC algorithm can be expressed as

$$\min_{X,U} \sum_{i=0}^{N} \|y_i\|_{\tilde{Q}}^2 + \|[u_i^{\top} 1]^{\top}\|_{\tilde{R}}^2$$
s.t. $\forall i \in \mathbb{I}_0^{N-1}$ (23a)

s.t.
$$\forall i \in \mathbb{I}_0^{N-1}$$
 (23b)

$$x_{i+1} = A(\rho_i)x_i + B(\rho_i)u_i + \mathcal{W}_i^{\mathbf{x}}, \tag{23c}$$

$$y_i = C(\rho_i)x_i + \mathcal{W}_i^{\mathbf{y}},\tag{23d}$$

$$H^{\mathbf{x}}(\rho_i)x_i + H^{\mathbf{u}}(\rho_i)u_i + \mathcal{W}_i^{\mathbf{h}} \le 0, \tag{23e}$$

$$x_0 = x[k], (23f)$$

TABLE III: Comparison of the NMPC schemes for autonomous racing simulations. $T_{\rm prep}$ and $T_{\rm fb}$ are in ms.

Alg.	$(\tilde{x}_i, \ \tilde{u}_i)$	T_{prep}	$T_{ m fb}$	$\Delta r_{\rm avg}$	r_{avg}
SQP	_	13.7	9.21	0.77	3.45
LPV	(0, 0)	17.6	9.4	0.65	3.23
LPV	$(c^{\mathrm{x}}, c^{\mathrm{u}})$	17.6	9.3	0.61	3.33
LPV	(x[k], u[k-1])	17.6	9.4	0.60	3.19
LPV	$(\hat{x}_i, \ \hat{u}_i)$	17.6	9.4	0.77	3.45

where \tilde{Q} is the weighting matrix of the contouring and lag error and \tilde{R} is the input weighting matrix as outlined in [14].

3) Simulation Results: In the following simulations, we compare how the LPV-MPC and the SQP algorithms perform in an RTI scheme. The simulations are performed using the simulator module of CRS [21], which uses the dynamic model of a 1/28 scale autonomous electrical car.

During the simulation experiments, we execute multiple laps around a test track with the controller and compare the average KKT residuals and the residual reduction after each iteration, which is computed as the ratio between the residuals after and before $(\Delta r_{\rm avg} = \sum_0^{N_{\rm sim}} \frac{r_{k+1}}{r_k}/N_{\rm sim})$ each QP solution step. Furthermore, we compare the average preparation and feedback times of the RTI iterations. Note that, since we do not have access to the optimal solution, we omit case (5) from this study.

As shown in Table III, the SQP method achieves shorter preparation times than the iterative LPV-MPC, because the Jacobians are evaluated only once per step along the prediction horizon, whereas the LPV-MPC requires multiple evaluations for numerical integration. Given that the resulting QPs have similar structures, the feedback times are comparable. However, LPV-MPC generally exhibits a larger average reduction in NLP residuals and a smaller average residual value. This indicates that the LPV-MPC algorithm tends to operate closer to optimality in the RTI framework. Lastly, note that with a suitable selection of anchor points, the SQP and LPV-MPC iterations become equivalent.

V. EXPERIMENTS

We conduct real-world experiments by applying learning-based MPCC on the small-scale vehicle platform, allowing us to evaluate the zero-order approximations scheme⁶. The setup is based on CRS [21], which employs custom 1/28-scale electric cars and a Qualisys motion capture system. As in simulation, the controller is formulated as an MPCC (Sect. IV-B.2), but in experiments, we augment the nominal model with a GP to learn the residual dynamics inherently present when working with real hardware. Then, we utilize the stochastic GP-MPC scheme of [12].

Formally, we consider $x[k+1] = f_{\mathbf{C}}(x[k], u[k]) + B_{\mathbf{g}}g(x[k], u[k]) + w[k]$, where w[k] is the process noise, $g: \mathbb{R}^{n_{\mathbf{x}}} \times \mathbb{R}^{n_{\mathbf{u}}} \to \mathbb{R}^{n_{\mathbf{g}}}$ is the unknown residual dynamics and $B_{\mathbf{g}} \in \mathbb{R}^{n_{\mathbf{x}} \times n_{\mathbf{g}}}$ is a full column rank matrix, characterizing that g only affects a subspace of the full state space. As most significant modeling errors usually appear

TABLE IV: Comparison of the MPCC implementations in real hardware experiments. Times are in milliseconds.

Alg.	$T_{\rm sol}$	T_{prep}	$T_{ m fb}$	Cost	Safe
LPV	20.54	17.60	2.93	5.53	
SQP	5.13	2.17	2.95	4.37	
GP-LPV	31.31	25.83	5.45	6.88	√
GP-SQP	23.72	18.63	5.07	7.46	√

in the tire and drivetrain parameter estimates [14], [23], we define $B_{\rm g} \doteq [0_{3\times3} \ I_{3\times3} \ 0_{3\times3}]^{\rm T}$ and estimate g with GPs, i.e., $g \sim \mathcal{GP}(\mu_{\rm g}, \Sigma_{\rm g})$, where $g: \mathbb{R}^{n_{\rm x}} \times \mathbb{R}^{n_{\rm u}} \to \mathbb{R}^{n_{\rm g}}$ is the posterior mean and $\Sigma_{\rm g}: \mathbb{R}^{n_{\rm x}} \times \mathbb{R}^{n_{\rm u}} \to \mathbb{R}^{n_{\rm g}\times n_{\rm g}}$ is the posterior variance. As the computational demand of the naive GP-MPC scales quadratically with the number of system states, we utilize the zero-order approximation (Sec. III-B) for the propagation of covariances. The formulation and implementation of the GP-MPC for autonomous racing are based on [12], [14].

The GP implementation is based on the GPYTORCH package and uses D=50 datapoints collected and updated online according to [14, Sec. IV.D.2]. The controller is run in RTI-mode at 30 Hz, with a prediction horizon of N=40. To compute the integrals (9), we use the Gauss-Legendre scheme with $n_{\rm nom}^{\rm int}=40$ for the nominal model and $n_{\rm GP}^{\rm int}=20$ for the GPs. In the experiments, we compare four schemes: nominal (1) SQP and (2) LPV using the measured state and the last input as anchor points, (3) zero-order GP-SQP and (4) zero-order GP-LPV.

As shown in Fig. 3 and Table IV, the nominal controllers guide the car around the track but fail to follow the optimal raceline. During testing, manual safety margin in the form of tightened track constraints ($d_{\rm t}=0.02~{\rm m}$) are needed in this case to prevent collisions, whereas the GP-MPCC schemes operated safely without such adjustments, as indicated by the Safe column in Table IV. In terms of computation, SQP is faster, as it only evaluates Jacobians (5) N times, while the LPV method requires $N(n_{\rm nom}^{\rm int}+n_{\rm GP}^{\rm int})$ evaluations for numerical integration. Although parallelization mitigates this, SQP remains more efficient in RTI schemes. However, in the learning-based setting, the LPV-MPC attains a lower average cost due to improved model approximations. This is in contrast to the nominal case, where the average cost is higher, because the mismatch has a more significant effect.

VI. CONCLUSION

In this paper, we presented a unified solution method for NMPC problems that integrates SQP and LPV-MPC algorithms as subcases. Specifically, we showed that by the appropriate choice of the sensitivity matrices, both algorithms can be implemented within a common framework, for which we provide an open-source implementation. In particular, we showed that the FTC embedding for LPV-MPC recovers SQP under a specific choice of anchor points. Furthermore, we integrated the zero-order Jacobian approximation into the unified framework and showed its connection to LPV scheduling variables. Finally, in numerical simulations, we highlighted their convergence properties and computational

 $^{^6}$ Experimental data available: doi:10.3929/ethz-c-000787107

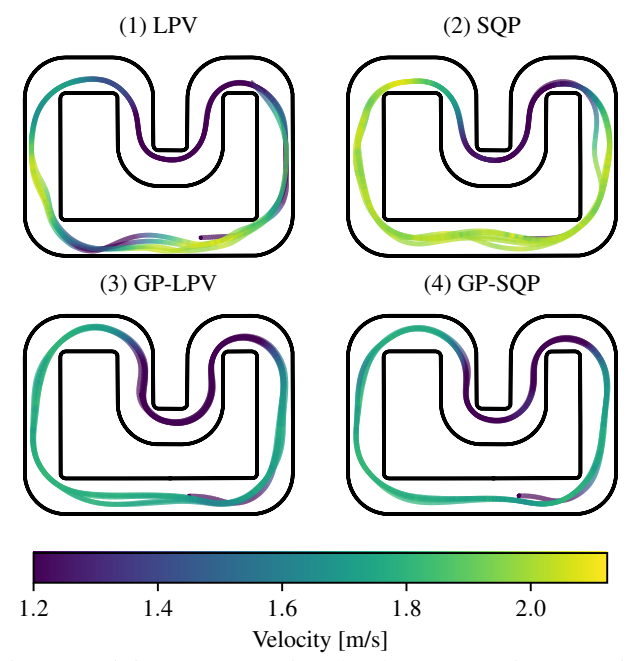


Fig. 3: Miniature car racing hardware experiments with the MPCC implementations. A video of the experiments is available at https://youtu.be/-zPCEP9Ahok.

complexity and deployed both algorithms in real-world experiments for autonomous racing.

REFERENCES

- J. B. Rawlings, D. Q. Mayne, and M. Diehl, Model Predictive Control: Theory, Computation, and Design, 2nd ed. Nob Hill Publishing, 2017.
- [2] J. A. E. Andersson, J. Gillis, G. Horn, J. B. Rawlings, and M. Diehl, "Casadi: a software framework for nonlinear optimization and optimal control," *Math. Prog. Comp.*, vol. 11, no. 1, p. 1–36, Mar. 2019.
- [3] J. Nocedal and S. J. Wright, *Numerical optimization*, 2nd ed., ser. Springer series in operations research. New York: Springer, 2006.
- [4] D. Kouzoupis, G. Frison, A. Zanelli, and M. Diehl, "Recent advances in quadratic programming algorithms for nonlinear model predictive control," *Vietnam J. Math.*, vol. 46, no. 4, p. 863–882, Dec. 2018.
- [5] M. Diehl, "Real-time optimization for large scale nonlinear processes," Ph.D. dissertation, Ruprecht-Karls-Universitat Heidelberg, 2001.
- [6] P. S. Gonzalez Cisneros, "Quasi-linear model predictive control: Stability, modelling and implementation," Ph.D. dissertation, Technische Universitat Hamburg, 2021.
- [7] C. Hespe and H. Werner, "Convergence properties of fast quasi-lpv model predictive control," in *Prof. Conf. Decis. Control (CDC)*, Dec. 2021, p. 3869–3874.
- [8] J. H. Hoekstra, B. Cseppento, G. I. Beintema, M. Schoukens, Z. Kollár, and R. Tóth, "Computationally efficient predictive control based on ANN state-space models," in *Proc. Conf. Dec. Control (CDC)*, 2023, p. 6336–6341.
- [9] E. J. Olucha, P. J. Koelewijn, A. Das, and R. Tóth, "Automated linear parameter-varying modeling of nonlinear systems: A global embedding approach," *IFAC-PapersOnLine*, vol. 59, no. 15, pp. 49–54, 2025.
- [10] X. Feng, S. D. Cairano, and R. Quirynen, "Inexact adjoint-based sqp algorithm for real-time stochastic nonlinear mpc," *IFAC-PapersOnLine*, vol. 53, no. 2, p. 6529–6535, 2020.
- [11] A. Zanelli, J. Frey, F. Messerer, and M. Diehl, "Zero-order robust nonlinear model predictive control with ellipsoidal uncertainty sets," *IFAC-PapersOnLine*, vol. 54, no. 6, p. 50–57, 2021.
- [12] A. Lahr, A. Zanelli, A. Carron, and M. N. Zeilinger, "Zero-order optimization for gaussian process-based model predictive control," *Eur. J. Control*, vol. 74, p. 100862, Nov. 2023.
- [13] P. Polcz, T. Péni, and R. Tóth, "Efficient implementation of gaussian process-based predictive control by quadratic programming," *IET Control Theory & Appl.*, vol. 17, no. 8, p. 968–984, 2023.

- [14] A. Lahr, J. Näf, K. P. Wabersich, J. Frey, P. Siehl, A. Carron, M. Diehl, and M. N. Zeilinger, "L4acados: Learning-based models for acados, applied to gaussian process-based predictive control," no. arXiv:2411.19258, Nov. 2024.
- [15] P. T. Boggs and J. W. Tolle, "Sequential quadratic programming," Acta Numerica, vol. 4, p. 1–51, Jan. 1995.
- [16] H. S. Abbas, R. Tóth, M. Petreczky, N. Meskin, and J. Mohammad-pour, "Embedding of nonlinear systems in a linear parameter-varying representation," *IFAC Proc. Vol.*, vol. 47, no. 3, pp. 6907–6913, 2014, 19th IFAC World Cong.
- [17] D. S. Karachalios and H. S. Abbas, "Efficient nonlinear model predictive control by leveraging linear parameter-varying embedding and sequential quadratic programming," no. arXiv:2403.19195, Mar. 2024
- [18] S. Gros, M. Zanon, R. Quirynen, A. Bemporad, and M. Diehl, "From linear to nonlinear mpc: bridging the gap via the real-time iteration," *Int. J. Control*, vol. 93, no. 1, pp. 62–80, 2020.
- 19] K. Guemghar, B. Srinivasan, P. Mullhaupt, and D. Bonvin, "Predictive control of fast unstable and nonminimum-phase nonlinear systems," in *Proc. Amer. Control Conf. (ACC)*, vol. 6, 2002, pp. 4764–4769 vol.6.
- [20] L. Hewing, J. Kabzan, and M. N. Zeilinger, "Cautious model predictive control using gaussian process regression," *IEEE Trans. Control Syst. Technol.*, vol. 28, no. 6, p. 2736–2743, Nov. 2020.
- [21] A. Carron, S. Bodmer, L. Vogel, R. Zurbrügg, D. Helm, R. Rickenbach, S. Muntwiler, J. Sieber, and M. N. Zeilinger, "Chronos and crs: Design of a miniature car-like robot and a software framework for single and multi-agent robotics and control," in *Prof. Int. Conf. Robot. Autom.*, May 2023, p. 1371–1378.
- [22] L. Hewing, A. Liniger, and M. N. Zeilinger, "Cautious nmpc with gaussian process dynamics for autonomous miniature race cars," in *Eur. Control Conf. (ECC)*, 2018, p. 1341–1348.
- [23] K. Floch, T. Péni, and R. Tóth, "Gaussian-process-based adaptive trajectory tracking control for autonomous ground vehicles," in *Proc. Eur. Control Conf. (ECC)*, 2024, pp. 464–471.

APPENDIX

A. Hessian Approximations in SQP

The Lagrangian of the NMPC (2) can be expressed as

$$\mathcal{L}(X, U, \Theta, \mathcal{N}) = \sum_{i=0}^{N-1} \left(l_i(x_i, u_i) + \vartheta_{i+1}^{\top}(f(x_i, u_i) - x_{i+1}) \right)$$

$$+\mu_i^{\top} h(x_i, u_i) + l_N(x_N) + \mu_N^{\top} h(x_N, u_N) + \vartheta_0(x_0 - x[k]),$$
(24)

where $\Theta = [\vartheta_0^\top \dots \vartheta_N^\top]^\top$ and $\mathcal{N} = [\mu_0^\top \dots \mu_N^\top]^\top$ are the Lagrange multipliers corresponding to the inequality and the equality constraints, respectively.

Using the exact Hessian of the Lagrangian, M_i is calculated as

$$\mathcal{M}_0 = \nabla_{(x_0, u_0)}^2 \mathcal{L} = \nabla^2 l_0 + \vartheta_0^\top \operatorname{diag}(\mathbf{I}_{\mathbf{n_x} \times \mathbf{n_x}}, \mathbf{0}_{\mathbf{n_u} \times \mathbf{n_u}}) + \mu_0^\top \nabla^2 h(x_0, u_0),$$
(25)

$$\mathcal{M}_{i} = \nabla_{(x_{i}, u_{i})}^{2} \mathcal{L} = \nabla^{2} l_{i} + \vartheta_{i}^{\mathsf{T}} \nabla^{2} f(x_{i}, u_{i})$$

$$+ \mu_{i}^{\mathsf{T}} \nabla^{2} h(x_{i}, u_{i}), \quad \forall i \in \mathbb{I}_{1}^{N-1},$$
(26)

$$\mathcal{M}_N = \nabla^2_{(x_N, u_N)} \mathcal{L} = \nabla^2 l_N + \mu_N^\top \nabla^2 h(x_N, u_N). \tag{27}$$

Under the Gauss-Newton approximation the Hessian of the Lagrangian for quadratic cost (3) is $\nabla^2_{(x_i,u_i)}\mathcal{L}\approx \nabla^2_{(x_i,u_i)}l_i(x_i,u_i)$, i.e., the constraint curvature terms are neglected. Therefore,

$$\mathcal{M}_i = \nabla^2_{(x_i, y_i)} \mathcal{L} = \operatorname{diag}(Q, R), \quad i \in \mathbb{I}_0^{N-1}$$
 (28)

$$\mathcal{M}_N = \nabla^2_{(x_N, u_N)} \mathcal{L} = W. \tag{29}$$